JOURNAL OF CATALYSIS 87, 265–275 (1984)

Gold–Titania Interactions: Temperature Dependence of Surface Area and Crystallinity of TiO_2 and Gold Dispersion

A. G. SHASTRI, A. K. DATYE, AND J. SCHWANK[1]

Department of Chemical Engineering, The University of Michigan, Ann Arbor, Michigan 48109

Received August 1, 1983; revised November 17, 1983

The influence of temperature on the BET surface area, crystallinity, and anatase/rutile phase transformation of blank TiO_2 and Au/TiO_2 catalysts is studied. Presence of gold delays the recrystallization of anatase and the phase transformation into rutile. In turn, high gold dispersions are stabilized by TiO_2 up to a temperature of 700°C. Agglomeration of gold into large particles coincides with the phase transformation into rutile at 800°C. The stability of the gold dispersion does not seem to be due to an SMSI effect. The low metal loading used to impregnate a high-surface-area TiO_2 may be responsible for either an incorporation of gold atoms in interstitial positions of the TiO_2 lattice, or the trapping of small gold particles in micropores.

INTRODUCTION

Recent studies have shown that Group VIII noble metals supported on TiO_2, V_2O_3, and Nb_2O_5 exhibit a strong metal–support interaction (SMSI) effect which is manifested by suppression of hydrogen and carbon monoxide chemisorption following H_2 reduction at high temperature. The SMSI effect is believed to be related to the ease of reducibility of the support material (*1*). Oxides resisting reduction by H_2 such as SiO_2 or Al_2O_3 do not exhibit the SMSI effect. The Pt/TiO_2 system has been extensively studied with respect to catalytic activity and chemisorption properties (*2–6*). Under SMSI conditions, a pillbox morphology for Pt crystallites was observed along with a remarkable stability of metal dispersion at elevated temperatures. *In situ* investigation of the electrical conductivity of Pt/TiO_2 catalysts indicated that during reduction at high temperature, spillover of atomic hydrogen from Pt sites to the TiO_2 support took place resulting in formation of Ti_4O_7. The platinum was found to be markedly enriched in electrons under these conditions resulting in suppression of chemisorption and catalytic activity due to filling of the platinum *d* orbitals (*7*).

In view of the above observations, it was of interest to examine the behavior of gold supported on TiO_2. Gold, although similar in electronic structure to platinum, is not capable of dissociating molecular hydrogen except at very high temperatures. Hence, in contrast to platinum, one would not expect the presence of SMSI effects in the Au/TiO_2 system. The emphasis of this study was to explore the effect of thermal treatment on both gold dispersion as well as on surface area and phase transformations in TiO_2. The dispersion of gold was measured by chemisorption of oxygen at 200°C. For comparison, carbon monoxide adsorption at 50°C was attempted. In view of the uncertainties regarding the chemisorption stoichiometry of gases on gold, metal dispersions were also determined by electron microscopy and wide-angle X-ray scattering (WAXS).

EXPERIMENTAL

The Glidden TiO_2 used as support for the gold catalysts was prepared by hydrolysis of titanium isopropylate, followed by washing and drying at 105°C under vacuum.

[1] Author to whom correspondence should be addressed.

0021-9517/84 $3.00

Based on wide-angle X-ray scattering results, the support consisted of pure anatase. No peaks characteristic of the rutile phase of TiO_2 were found.

The support was impregnated with an aqueous solution of reagent grade $HAuCl_4 \cdot 3H_2O$ (Baker), dried at 110°C for 2 hr, and reduced for 4 hr at 390°C. Neutron activation analysis of the Au/TiO_2 catalyst gave a gold content of 0.636 wt%, with only a trace of chlorine (0.01 wt%). Aliquots of the catalyst were subjected to a thermal treatment routine. Each aliquot was placed into a Pyrex glass reactor loop and gradually heated in a stream of flowing N_2 gas to the treatment temperature. The temperature was kept constant for 2 hr followed by a slow cooling to room temperature. The samples so obtained were then used for further experimentation.

BET surface areas were determined by the single-point method using a Quantachrome Monosorb surface area analyzer. A mixture of 30% N_2 in He gas was used, with N_2 as adsorbent at a temperature of −195.8°C. WAXS experiments were performed after each thermal treatment in a Philips X-ray powder diffractometer. Ni-filtered CuK_α radiation was used. Crystallite sizes were calculated by Scherrer's equation taking into consideration the corrections for instrumental line broadening.

Electron microscopy studies were carried out using a JEOL JEM-100CX microscope. For high resolution work, a top-entry stage, a UHP pole piece, and a LaB_6 emitter were used. Microanalytical work under medium resolution was performed using a side-entry goniometer stage with a tungsten filament as electron source. The scanning capability was provided by an ASID-4D attachment. Elemental analysis by X-ray energy dispersive spectroscopy was carried out using a solid-state PGT detector interfaced with a Nuclear Data ND6620 computer.

Chemisorption experiments were performed in a Pyrex glass high vacuum static volumetric system using 0.2 to 0.4 g of catalyst. All the gases used for pretreatment and chemisorption were of research grade purity. The system was equipped with a three-stage Hg-diffusion pump, backed by a roughing pump. Several traps at liquid nitrogen temperature and gold wires were placed in strategic positions throughout the chemisorption apparatus to prevent Hg vapor and other impurities from entering the chemisorption system. Pressures in the range of 10^{-10} to 10^{-3} Torr (1 Torr = 133.3 N m^{-2} were measured by a Veeco ionization gauge. From 10^{-3} to 20 Torr, a calibrated Televac thermocouple gauge was employed. Pressures 0–260 Torr were measured by a Wallace-and-Tiernan digital gauge. A high-precision McLeod gauge with a range from 10^{-5} to 25 Torr was used for calibration purposes. The temperature of the adsorption zone was kept constant within ± 1°C. Dead volumes in the adsorption system were determined by expanding helium from a calibrated glass burette.

For CO adsorption, the samples were pretreated for 16 hr in 125 Torr of hydrogen at 250°C. The reactor was then evacuated and a second dose of hydrogen at the same temperature and pressure was introduced for another 2 hours. This procedure was followed by evacuation to about 10^{-5} Torr and cooling to the desired adsorption temperature. Carbon monoxide adsorption isotherms were measured at 50°C, using pressures in the range of 0.5 to 10 Torr. For each gas uptake, 30 min of equilibration time was allowed.

For oxygen chemisorption, the pretreatment procedure was changed. Since H_2 pretreatment could cause the reduction of some of the TiO_2 support, leading to erroneously increased oxygen uptake values in the chemisorption, H_2 was avoided altogether. Instead, the samples were exposed to 50 Torr of oxygen for 16 hr at 250°C, followed by brief evacuation and another dose of oxygen at the same temperature and pressure for 2 hr. The adsorption chamber was then evacuated and the reactor cooled to room temperature under dynamic

vacuum and kept there for 2 hr. Finally, the temperature was raised to 200°C under dynamic vacuum of 10^{-5} Torr. Chemisorption of oxygen was performed at 200°C in the pressure range of 0.5–10 Torr.

RESULTS AND DISCUSSION

This section addresses first the changes in BET surface area of blank TiO_2 and possible phase transformation from anatase to rutile as a consequence of thermal treatment. The results on blank TiO_2 are then compared to the Au/TiO_2 catalysts with main emphasis on effects of gold on the surface area changes and phase transformation. Finally, we discuss the capability of TiO_2 to stabilize high dispersion of Au particles in view of the current interest in SMSI.

Surface Area Changes in TiO_2 as a Function of Thermal Treatment

The BET results on TiO_2 used in the catalyst preparation showed an initial high surface area of 118 m^2/g at room temperature. Upon heating to 300°C the surface area increased slightly followed by a sharp reduction to approximately 2.7 m^2/g at 600°C (Fig. 1). Such low surface areas are typical for the rutile form of TiO_2. For example, a high purity rutile (Glidden) had a low initial surface area of approximately 1.7 m^2/g which remained constant after thermal treatments up to 600°C (Fig. 1).

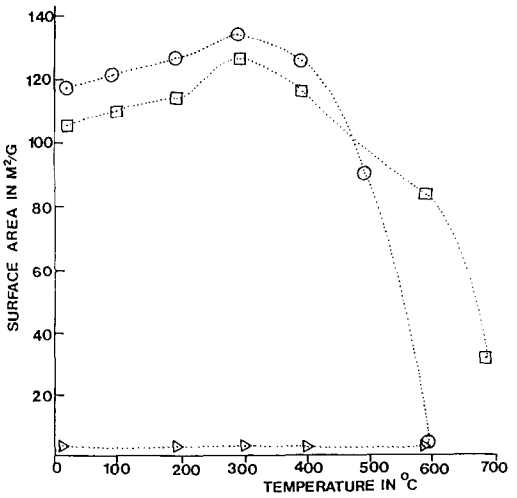

FIG. 1. BET surface area as a function of pretreatment temperature. ○ Blank TiO_2 used for gold catalyst preparation; □ Au/TiO_2; △ high purity rutile.

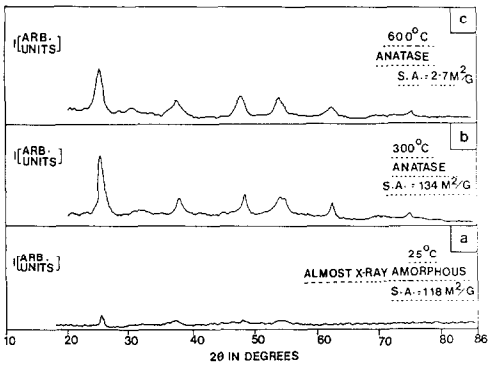

FIG. 2. WAXS patterns of TiO_2 used for catalyst preparation as a function of thermal pretreatment. (a) Fresh sample; (b) after heating to 300°C for 2 hr; (c) after heating to 600°C for 2 hr.

The question now arises as to whether the collapse in surface area of the TiO_2 support is due to a phase transformation into low surface area rutile or due to the formation of a more crystalline phase. To answer this question, WAXS patterns of TiO_2 as a function of thermal treatment were obtained (Fig. 2). The fresh TiO_2 sample having a surface area of 118 m^2/g had small peaks in quite similar positions to those for anatase. This sample, although almost X-ray amorphous, was found to be microcrystalline. High-resolution electron microscopy showed domains of approximately 200 Å in diameter exhibiting regular lattice fringes (see Fig. 7). Most of these domains corresponded to anatase. However, a few of these domains had lattice fringes typical for the brookite phase of titania (example: the most clearly visible lattice fringes in Fig. 7 happen to be brookite lattice fringes). After treatment at 300°C a surface area of 134 m^2/g was measured and X-ray diffraction patterns characteristic of the anatase phase were observed. Even after treatment at 600°C where the surface area had decreased to 2.7 m^2/g, the diffraction pattern was clearly that of anatase. No rutile peaks

were observed. This convincingly proves that the collapse in surface area is not due to the phase transformation to rutile but rather due to the growth of larger anatase crystallites. Only after treatment at 700°C for 2 hr was a phase-transformation to rutile observed (see Fig. 4). This is consistent with previous findings that thermal treatment of titania gel caused the disappearance of micropores and a sharp decrease in surface area at 600°C accompanied by a transition from an X-ray amorphous state into highly crystalline anatase (*8*). A similar recrystallization of an initially amorphous structure was observed by Baker *et al.* on heating of thin TiO_2 films in H_2 up to 552°C. However, after heating to 802°C, a complete transformation to rutile was observed (*3*). The kinetics of the anatase to rutile transformation has been extensively studied by several investigators (*9–14*).

Influence of Au

The Au/TiO_2 sample had a BET surface area similar to that of blank TiO_2 (Fig. 1). However, thermal treatment at higher temperatures did not reduce the surface area of Au/TiO_2 as drastically as in the case of blank TiO_2. Even at 700°C, the surface area of Au/TiO_2 remained relatively high (34 m^2/g). Figure 3 shows the WAXS patterns of the Au/TiO_2 catalyst obtained after various thermal treatments. No peaks that could be attributed to Au were observed; even after treatment at 700°C all the observed peaks were due to the presence of a crystalline anatase phase. It should be noted that the Au/TiO_2 sample clearly showed anatase peaks at 25°C, where the blank TiO_2 had been almost X-ray amorphous. This difference might be due to the fact that the gold catalyst preparation included a reduction step at 390°C. The impregnation of TiO_2 with gold prevented to some extent the collapse of the TiO_2 surface area at temperatures of 600 to 700°C. Gold also exhibited a retarding effect on the anatase to rutile phase transformation. On blank TiO_2, a complete phase transformation had occurred within 2 hr at 700°C, while Au/TiO_2 did not transform at all under these conditions. On Au/TiO_2 samples, a complete phase transformation from anatase to rutile was observed after a treatment at 800°C for 20 hr (Fig. 4). From previous work it is known that the kinetics of the phase transformation can be influenced by the presence of substitutional or interstitial foreign ions (*12–14*). Adding metal oxides to TiO_2 can accelerate the phase transformation (*10, 11*). This appears to be related to the creation of oxygen vacancies in the TiO_2 lattice as a consequence of metal ions such as Cu^{2+} and Co^{2+} that are present in substitutional positions (*12*). One might,

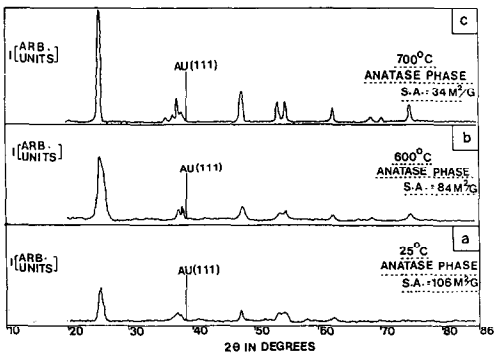

FIG. 3. WAXS patterns of Au/TiO_2 as a function of thermal pretreatment. (a) Fresh sample; (b) after heating to 600°C for 2 hr; (c) after heating to 700°C for 2 hr.

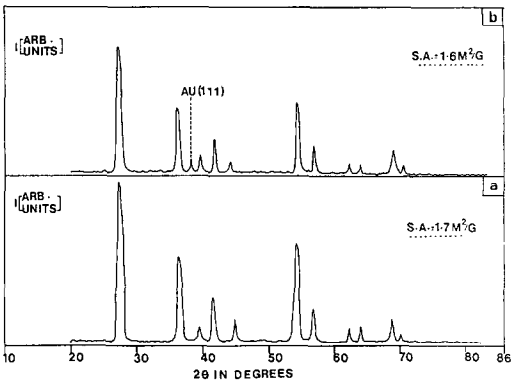

FIG. 4. (a) WAXS patterns of blank TiO_2 used for catalyst preparation after heating to 700°C in air for 2 hr. (b) WAXS patterns of Au/TiO_2 after heating to 800°C for 20 hr in air (anatase to rutile transformation).

therefore, expect a similar accelerating effect if some of the gold was present in the form of substitutional cations.

If, on the other hand, Au atoms or ions were located in interstitial positions in the titania lattice, an inhibiting effect on the phase transformation of anatase to rutile should be expected (*11*, *12*). The latter case was experimentally observed in the present study. This suggests that part of the gold might be occupying interstitial positions in the TiO_2 lattice. Since there is to the best of our knowledge no previous fundamental study of the Au/TiO_2 system, verification of this hypothesis has to await further study.

Dispersion of Au as a Function of Thermal Treatment

As a measure for gold dispersion and average particle size, the chemisorption of O_2 was carried out. Figure 5 shows adsorption isotherms for O_2 on Au/TiO_2. These isotherms are based on the irreversible uptake of the adsorbate. Under identical pretreatment and experimental conditions, the irreversible O_2 uptake by the blank TiO_2 was negligible. Monolayer adsorption volume was estimated by extrapolating the linear portion of the isotherm to zero pressure. In the fresh Au/TiO_2 sample the uptake of oxygen did not level off as in the other cases involving high temperature treatment. Hence, the linear extrapolation in the fresh sample represents the most conservative estimate of oxygen uptake. Looking at the isotherms it cannot be excluded that the fresh sample had even higher dispersion than the samples treated at higher temperatures. For O_2 chemisorption at 200°C, a stoichiometry of four gold sites per oxygen molecule was assumed. This stoichiometry has been previously proposed for O_2 chemisorption at 200°C on Au/SiO_2, Au/MgO, and Au/Al_2O_3 samples and gave results that were in good agreement with TEM and WAXS data (*15*).

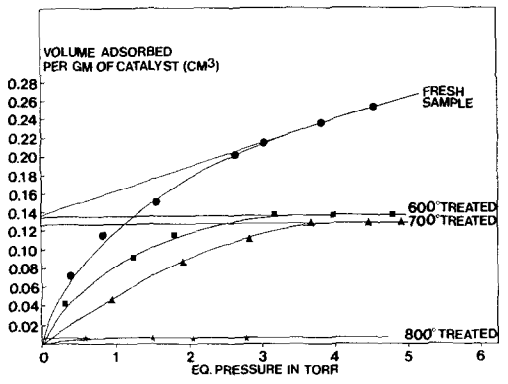

FIG. 5. Oxygen adsorption isotherms on Au/TiO_2 at 200°C after heating aliquots of the sample to different temperature, followed by the standard oxygen pretreatment described in the text. The volume of gas irreversibly adsorbed is corrected to STP. The "fresh" sample was only subjected to the standard pretreatment at 250°C.

In view of the many open questions and uncertainties involving oxygen adsorption on gold surfaces, a second adsorbate, namely CO, was employed for comparison. Previous infrared results indicated that CO can adsorb on gold in a linear mode (*16*, *17*). This would correspond to a Au/CO stoichiometry of 1/1. Blank TiO_2 showed some uptake of CO at room temperature. With increasing temperature, the uptake of CO decreased and became negligible at 50°C. Therefore, the CO adsorption on Au/TiO_2 was carried out at 50°C. Adsorption of CO was found to be weak and completely reversible (Fig. 6). Upon evacuation for 5 min, all the CO could be completely removed from the catalyst. The CO data agree remarkably well with the oxygen chemisorption data if we tentatively assume that the Au/CO stoichiometry is 1/1 and that we were able to come close to monolayer coverage on gold at CO partial pressures of 7 Torr or higher. The average particle size, d, of gold was calculated, using the relation $d = 6/S\rho$, where S is the surface area and ρ is the density of gold. The cross-sectional area of one gold surface atom was estimated to be equal to 9.13 $Å^2$. Table 1 summarizes the results for particle size and dispersion for both O_2 and CO adsorption.

O_2 chemisorption on a fresh Au/TiO_2 catalyst gave a dispersion of 75%. CO adsorp-

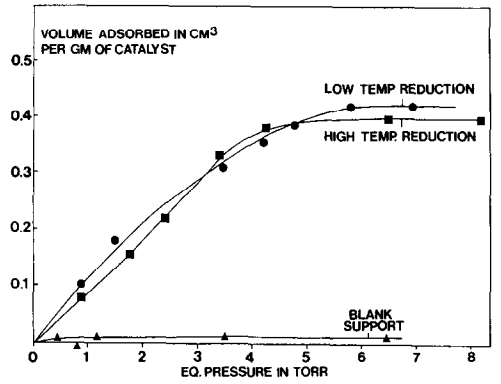

FIG. 6. CO adsorption isotherms on Au/TiO_2 at 50°C after low-temperature (250°C), and high-temperature (500°C) reduction in H_2. The volume of gas reversibly adsorbed is corrected to STP.

tion based on the previous assumptions would give a dispersion of 67%. Table 1 shows that there was no significant agglomeration of gold up to 700°C. However, after treatment at 800°C, a massive drop in both O_2 and CO uptake is observed. These findings are supported by WAXS where no gold peaks could be found up to 700°C (Fig. 3), while the 800°C treated sample showed sharp gold peaks (Fig. 4b). The mean gold particle size for the latter sample, based on WAXS was about 390 Å, in good agreement with chemisorption results (Table 1). It should, however, be noted that our WAXS results represent a volumetric average, while the particle size derived from chemisorption experiments is weighted with respect to the gold surface area. The observed decrease in gas uptake after treatment at 800°C is not directly related to changes in the BET surface area. The BET surface area at 700°C was already down to 29% of the original area while the O_2 and CO uptake remained virtually unchanged. These facts along with the good agreement with WAXS data and the inability of the blank TiO_2 to chemisorb O_2 at 200°C and CO at 50°C under our pretreatment conditions indicate that the chemisorption takes place probably on gold sites, and not on the TiO_2 support.

There are two possible explanations for the absence of Au peaks in the X-ray diffraction patterns up to 700°C, namely a metal loading below the detection limit or a mean Au particle size of less than 40 Å. Therefore, the samples were further characterized by electron microscopy using an experimental technique reported previously (*18*). Under high-resolution conditions, no evidence for Au particles was found in the samples that had been treated up to 600°C (Fig. 7). Knowing the limitation of high-resolution electron microscopy which allows a look only at the thinnest regions of the specimen, any agglomeration into large Au particles in thicker areas of the sample might go unnoticed. Therefore, scanning transmission electron microscopy was used to investigate the thicker regions of the sample. Some dark regions with strong contrast could be seen. Such high contrast could be generated either by thick piles of TiO_2 or by large Au particles.

Scanning the electron beam over a region of approximately 3000 $Å^2$ resulted in a strong X-ray signal typical for Ti with only a faint Au signal (Fig. 8). Focusing the beam on certain areas of high contrast (100 Å in diameter), the ratio of the Au/Ti signal increased dramatically (Fig. 9). This provided positive identification of Au particles in the range of 100 Å or larger. No gold

TABLE 1

Chemisorption and WAXS Results[a]

Thermal treatment	O_2 chemisorption		CO adsorption[b]		WAXS d(Å)	Phase
	% D	d(Å)	% D	d(Å)		
250°C	75.2	15	66.8	17	n.d., <40	A
600°C	74	15	58.2	20	n.d., <40	A
700°C	71.4	16	45.2	25	n.d., <40	A
800°C	3.4	332	2.6	433	390	R
After H_2 reduction at 500°C	—	—	55.2	21	n.d., <40	A

[a] Thermal treatment at indicated temperature for 2 hr in N_2/He mixture. Samples at 700 and 800°C treated in air for 2 and 20 hr, respectively. This was followed by standard pretreatments for chemisorption described in the text. % D, Percentage dispersion; d, mean particle size; n.d., gold metal peak not detectable; A, anatase; R, rutile.

[b] Based on reversible uptake of CO, assuming monolayer coverage with 1/1 stoichiometry of Au/CO.

FIG. 7. High-resolution transmission electron micrograph of Au/TiO_2 (fresh sample).

particles smaller than 100 Å were seen. Figure 10 is a TEM picture of a typical area analyzed by EDS (see Figs. 8 and 9). This picture was taken prior to the STEM-EDS analysis. Under our conditions, pictures taken in the STEM mode are generally of poorer quality compared to TEM pictures. Our procedure consisted of first photo-

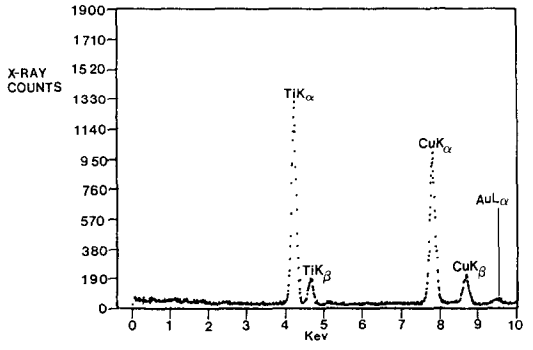

FIG. 8. X-Ray energy dispersive analysis (EDS) of a 3000 Å × 3000 Å region obtained in the scanning mode. Au/TiO_2 catalyst pretreated at 600°C. The Cu peaks arise from the grids used to support the sample.

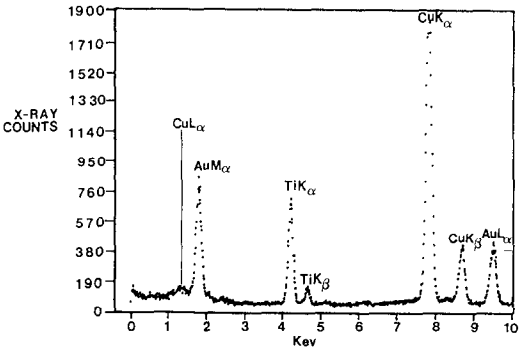

FIG. 9. X-Ray energy dispersive analysis (EDS) of Au/TiO_2 catalyst pretreated at 600°C. The 100-Å-diameter electron beam was focused on a dark region of the same area analyzed in Fig. 8. The increased Cu signal is due to electrons scattered from the gold particle.

graphing an area of interest in the TEM mode and then switching over to the STEM mode for elemental analysis. The sample treated at 600°C showed only a small number of gold particles similar to those seen in Fig. 10. Samples treated at 700°C exhibited a quite different morphology of the TiO_2 support due to its increased crystallinity. This made it more difficult to distinguish gold particles from TiO_2 crystallites (Fig. 11). After treating the sample at 800°C which resulted in phase transformation into rutile, the same problem was encountered. However, here the WAXS pattern clearly demonstrated the existence of large gold particles.

Our chemisorption results indicated a gold particle size of about 15 Å (Table 1). However, electron microscopy failed to detect such particles in any of our Au/TiO_2 samples. To resolve 15 Å gold particles in the high-resolution mode would be a fairly routine task with our microscope (*18*). It should be noted that Fig. 7 shows clearly resolved lattice fringes of TiO_2 (3.5 Å). There are several explanations for the discrepancy between chemisorption results and electron microscopy observations. First, one might be tempted to challenge the validity of the chemisorption results altogether in the light of the problems associated with gas chemisorption on Au surfaces. This explanation however, cannot reconcile the absence of WAXS peaks for gold up to 700°C followed by a sharp gold X-ray pattern after treatment at 800°C. If all of the gold was present in the form of 100 Å particles or larger (the only gold particles that could be seen in TEM), one would expect WAXS peaks for gold even in the fresh sample, and a much lower O_2 uptake.

The second explanation is based on the fact that chemisorption measures only an average particle size. If one invokes a bimodal Au particle size distribution with part of gold in the form of large particles

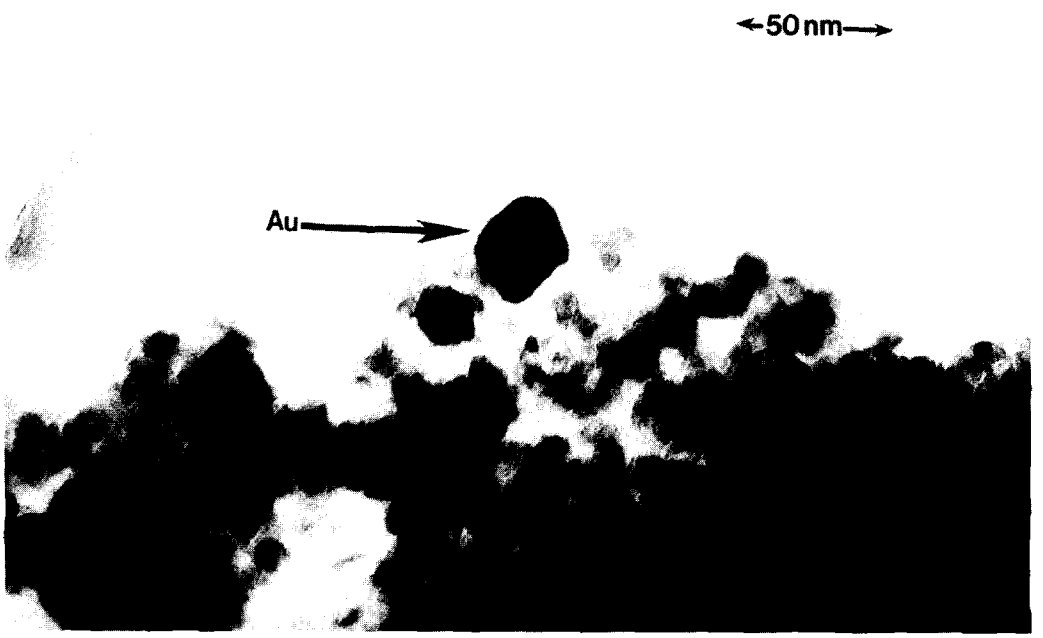

FIG. 10. TEM picture of Au/TiO_2 heated to 600°C.

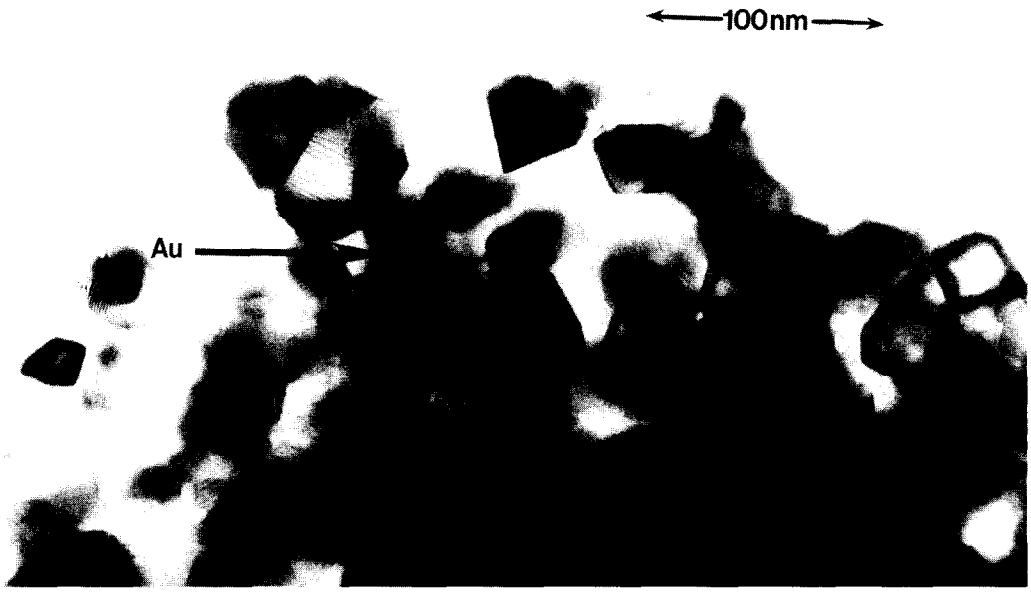

FIG. 11. TEM picture of Au/TiO_2 heated to 700°C.

(detectable in the microscope) and the remainder in a state of high, maybe even atomic dispersion, then one can easily account for the average Au dispersion observed in the chemisorption experiments. Bimodal distributions have been observed previously for supported Au catalysts (*19, 20*). In our case, we have seen a few 100–200 Å gold particles even in the sample treated at 250°C. The rest of the gold might be present in the micropores and in the interstitial lattice positions of TiO_2 and could account for the observed retardation in the anatase to rutile phase transformation of TiO_2. Such highly dispersed Au is probably beyond the detection limits of our high-resolution electron microscope.

The hypothesis of Au in interstitial positions of TiO_2 is further corroborated by the coincidence of massive gold agglomeration during the phase transformation to rutile as shown by WAXS and chemisorption. A study of the mechanism of the transformation has shown that anatase pseudo-closed-packed {112} planes of oxygen were retained as the rutile closed-packed {100} planes of oxygen in rutile. During the transformation a cooperative rearrangement of the titanium and oxygen ions occurs (*21*). The phase transformation also involves 8% shrinkage in molar volume of TiO_2. The mobility and consequent agglomeration of highly dispersed Au is expected to be significant during this process. A similar increase in metal particle size has also been observed in the Ni/TiO_2 system during the anatase-to-rutile phase transformation (*22*). It needs to be emphasized that the transition from X-ray amorphous TiO_2 to crystalline anatase and the changes in BET surface area upon heating up to 700°C has no major effect on the dispersion of gold. This result is remarkable in view of the sintering characteristics of gold on other oxide supports where due to its relatively low Tamman temperature, Au tends

to agglomerate readily into large particles upon heating. The TiO_2 support seems to have an exceptional capability to stabilize part of the gold in a state of high dispersion. However this stability of dispersion may not be due to a strong metal support interaction (SMSI) invoked for the Pt/TiO_2 system (*4–6*). Contrary to the findings in the Pt/TiO_2 system, no significant suppression of the CO uptake after reduction in hydrogen at 500°C was observed (Fig. 6). This result is not unexpected in view of the inability of Au to dissociate molecular hydrogen. The spillover of atomic hydrogen generated on metallic sites and a consequent reduction of TiO_2 to Ti_4O_7 appears to be a prerequisite for the SMSI effect. A similar absence of SMSI was previously observed in the Ag/TiO_2 system (*23, 24*).

CONCLUSIONS

This study has clearly demonstrated that TiO_2 plays a special role compared to other typical catalyst support materials. It can stabilize high dispersion of Au up to 700°C. This phenomenon does not appear to be due to the SMSI effect. While a temperature of 700°C was sufficient to accomplish the complete phase transformation of anatase to rutile in blank TiO_2, no transformation occurred under identical conditions on TiO_2 impregnated with Au.

Based on the WAXS, chemisorption, and electron microscopy results, a bimodal distribution of Au on TiO_2 is proposed. Part of the gold is present in the form of particles 100 Å in diameter or larger. Another part seems to exist in a state of high dispersion, which might either be atomic gold dissolved in interstitial lattice positions of the support or small gold clusters located in micropores of the TiO_2. Our catalyst preparation technique involving low metal loading, high surface area of the support, and mild reduction conditions would favor the formation of such highly dispersed gold. Moreover, this highly dispersed gold does not seem to be mobile on the support. Only after a complete restructuring of the anatase into rutile does this gold agglomerate into larger particles. Chemisorption of O_2 gave results in excellent agreement with WAXS and proved to be a viable tool to measure gold dispersion. CO adsorption on Au/TiO_2 was found to be in qualitative agreement with the oxygen chemisorption results. The uptake of CO was unchanged even after reduction in hydrogen at 500°C indicating an absence of SMSI effects.

ACKNOWLEDGMENTS

Acknowledgment is made to the Donors of the Petroleum Research Fund administered by the American Chemical Society for support of this research. The authors are also grateful for partial support of this work by the AMAX Foundation and the National Science Foundation.

REFERENCES

1. Tauster, S. J., and Fung, S. C., *J. Catal.* **55,** 29 (1978).
2. Ko, E. I., and Garten, R. L., *J. Catal.* **68,** 233 (1981).
3. Baker, R. T. K., Prestridge, E. B., and Garten, R. L., *J. Catal.* **56,** 390 (1979).
4. Tauster, S. J., Fung, S. C., and Garten, R. L., *J. Amer. Chem. Soc.* **100,** 170 (1978).
5. Horsley, J. A., *J. Amer. Chem. Soc.* **101,** 2870 (1979).
6. Baker, R. T. K., Prestridge, E. B., and Garten, R. L., *J. Catal.* **59,** 293 (1979).
7. Herrmann, J.-M., and Pichat, P., *J. Catal.* **78,** 425 (1982).
8. El-Akkad, T. M., *J. Colloid Interface Sci.* **76,** 67 (1980).
9. Sullivan, W. F., and Cole, S. S., *J. Amer. Ceram. Soc.* **42,** 127 (1959).
10. Rao, C. N. R., *Canad. J. Chem.* **39,** 498 (1961).
11. Shannon, R. D., *J. Appl. Phys.* **35,** 3414 (1964).
12. Shannon, R. D., and Pask, J. A., *J. Amer. Ceram. Soc.* **48,** 391 (1965).
13. Floerke, O. W., *Mitt. Ver. Deut. Emailfachleute* **6,** 49 (1958).
14. Lida, Y., and Ozaki, S., *J. Amer. Ceram. Soc.* **44,** 120 (1961).
15. Fukushima, T., Galvagno, S., and Parravano, G., *J. Catal.* **57,** 177 (1979).
16. Yates, D. J. C., *Colloid Interface Sci.* **29,** 194 (1969).
17. Schwank, J., Parravano, G., and Gruber, H. L., *J. Catal.* **61,** 19 (1980).
18. Schwank, J., Allard, L. F., Deeba, M., and Gates, B. C., *J. Catal.* **84,** 27 (1983).

19. Bassi, I. W., Lytle, F. W., and Parravano, G., *J. Catal.* **42,** 139 (1976).

20. Cocco, G., Enzo, S., Fagherazzi, G., Schiffini, L., Bassi, I. W., Vlaic, G., Galvagno, S., and Parravano, G., *J. Phys. Chem.* **83,** 2527 (1979).

21. Shannon, R. D., and Pask, J. A., *Amer. Mineralogist* **49,** 1707 (1964).

22. Burch, R., and Flambard, A. R., *J. Catal.* **78,** 389 (1982).

23. Baker, R. T. K., Prestridge, E. B., and Murrell, L. L., Proceedings Eight North American Meeting of Catalysis Society, Philadelphia, PA 1983.

24. Baker, R. T. K., *in* "Metal Support and Metal Additive Effects in Catalysis" (B. Imelik *et al.*, Eds.), p. 37. Elsevier, Amsterdam, 1982.